Aerosol and Air Quality Research, 16: 1105–1117, 2016

ISSN: 1680-8584 print / 2071-1409 online
doi: 10.4209/aaqr.2015.06.0413

Can We Trust Real Time Measurements of Lung Deposited Surface Area Concentrations in Dust from Powder Nanomaterials?

Marcus Levin[1,2*], Olivier Witschger[3], Sébastien Bau[3], Elzbieta Jankowska[4], Ismo K. Koponen[2], Antti J. Koivisto[2], Per A. Clausen[2], Alexander Jensen[2], Kristian Mølhave[1], Christof Asbach[5], Keld A. Jensen[2]

[1] *Department of Micro and Nanotechnology, Technical University of Denmark, Kgs. Lyngby, DK-2800, Denmark*
[2] *National Research Centre for the Working Environment, Lersø Parkallé 105, DK-2100 Copenhagen, Denmark*
[3] *Institut National de Recherche et de Sécurité, Rue du Morvan, FR-54500 Vandoeuvre les Nancy, France*
[4] *Centraly Instytut Ochrony Pracy – Państwowy Instytut Badawczy, Zakład Zagrożeń Chemicznych, Pyłowych i Biologicznych, ul Czerniakowska 16, PL-00701 Warsaw, Poland*
[5] *Institut für Energie- und Umwelttechnik (IUTA),47229 Duisburg, Germany*

ABSTRACT

A comparison between various methods for real-time measurements of lung deposited surface area (LDSA) using spherical particles and powder dust with specific surface area ranging from 0.03 to 112 m^2 g^{-1} was conducted. LDSA concentrations measured directly using Nanoparticle Surface Area Monitor (NSAM) and Aerotrak and were compared to LDSA concentrations recalculated from size distribution measurements using Electrical Low Pressure Impactor (ELPI) and Fast Mobility Particle Sizer (FMPS). FMPS and ELPI measurements were also compared to dust surface area concentrations estimated from gravimetrical filter measurements and specific surface areas.

Measurement of LDSA showed very good correlation in measurements of spherical particles (R^2 > 0.97, Ratio 1.0 to 1.04). High surface area nanomaterial powders showed a fairly reliable correlation between NSAM and Aerotrak (R^2 0.73–0.93) and a material-dependent offset in the ratios (1.04–2.8). However, the correlation and ratio were inconsistent for lower LDSA concentrations. Similar levels of correlation were observed for the NSAM and the FMPS for high surface area materials, but with the FMPS overestimating the LDSA concentration. The ELPI showed good correlation with NSAM data for high LDSA materials (R^2 0.87–0.93), but not for lower LDSA concentrations (R^2 0.50–0.72). Comparisons of respirable dust surface area from ELPI data correlated well (R^2 > 0.98) with that calculated from filter samples, but materials-specific exceptions were present.

We conclude that there is currently insufficient reliability and comparability between methods in the measurement of LDSA concentrations. Further development is required to enable use of LDSA for reliable dose metric and regulatory enforcement of exposure.

Keywords: Lung deposited surface area; Exposure assessment; Aerosol measurement; Dustiness.

INTRODUCTION

There is increasing evidence that the pulmonary toxicological response of ambient air-pollution and manufactured nanomaterials may, at least partially, be driven by the specific surface area dose of the test materials (Oberdorster, 2000; Maynard and Kuempel, 2005; Duffin *et al.*, 2007; Jacobsen *et al.*, 2009; Giechaskiel *et al.*, 2009; Donaldson *et al.*, 2013; Saber *et al.*, 2014). Therefore, it is of high interest to include airborne particle surface area measurements to offer a potentially more biologically relevant metric in exposure and risk assessment. To meet these new developments, it is also of interest to include surface area measurements in dustiness testing; the latter tests are performed to rank the ability of powders to generate dust and used in e.g., new modeling approaches and regulatory exposure assessment (BS EN:15051, 2006; Aitken *et al.*, 2011; Jensen *et al.*, 2015).

The surface area of airborne dust particles may be determined by either direct or indirect methods. There are currently no commercially available real-time methods to determine the geometric surface area concentration of

* Corresponding author.
Tel.: +4539165274; Fax: +4539165201
E-mail address: mle@nrcwe.dk

airborne particles. In principle the most correct method would be direct determination of the specific surface area on filters using the BET inert gas-adsorption technique. Even-though this method has been demonstrated (LeBouf *et al.*, 2011a; Lebouf *et al.*, 2011b), the method is in reality not yet straight-forward and changes could potentially occur in the aerosol during filter-sampling and storage that might change the surface area. Therefore, this method may not be generally applicable.

Another approach is to estimate the surface area concentrations based on airborne particle number size distributions assuming particle shape. Particle number-size-distributions can be measured using a range of different optical, aerodynamic, electrical mobility and charging techniques. Therefore, the comparability in these measurements and the reliability in conversions from number and volume concentrations metrics is still not well documented for non-spherical particles such as aggregates and agglomerates commonly observed in dustiness tests, covering a wide range of sizes from nano- to µm-size (Ibaseta and Biscans, 2007; Schneider and Jensen, 2008; Jensen *et al.*, 2009; Tsai *et al.*, 2009; Levin *et al.*, 2014; Koivisto *et al.*, 2015; Koponen *et al.*, 2015). Even in case of direct release from an airborne synthesis processes, primary particles can already start to agglomerate or aggregate in the reactor and may further coagulate at or very near the point of release with similar result (Makela *et al.*, 2009; Hämeri *et al.*, 2009; Schneider *et al.*, 2011; Koivisto *et al.*, 2012; Koivisto *et al.*, 2015). Measurements are therefore challenging when the aerosol structure is not known, because this in principle prevents the possibility to convert number-size-distribution measurements into reliable surface area values (Fissan *et al.*, 2013).

To overcome the uncertainties in size-distribution conversion, the lung deposited surface area (LDSA), i.e., the fraction of the total airborne particle geometric surface area concentration that would deposit in the human lung, of aerosols can be measured in real-time. Based on particle unipolar diffusion charging and subsequent current measurement with electrometers (Fissan *et al.*, 2007; Shin *et al.*, 2007), this principle is used by several instruments such as the Aerotrak (Aerotrak 9000, TSI inc, MN, USA) and the Nanoparticle Surface Area Monitor (NSAM 3550, TSI Inc, MN, USA). It should be noted that this surface area is not the same as the surface area determined by nitrogen or krypton gas-adsorption using the BET technique for powders (Bau *et al.*, 2010).

Recently, a few studies reported measurements comparing the results of different number size-distribution and surface area monitors challenged to equidimensional or spherical and aggregated particles. For aerosol monitors, Asbach *et al.* (2012) investigated the correlation between Aerotrak (Aerotrak 9000, TSI inc, MN, USA) and Fast Mobility Particle Sizer (FMPS 3091, TSI inc, MN, USA) with polydisperse aerosols of different sizes and morphologies (35 nm cubic NaCl, 190 nm spherical Di-Ethyl-Hexyl-Sebacat (DEHS) oil particles and 50 nm agglomerated soot particles; all modal diameters), and found good agreement (mostly within ± 15% difference) and correlation for NaCl ($R^2 \geq 0.985$) and soot ($R^2 \geq 0.997$) but poorer agreement for DEHS with deviations up to 50% ($R^2 \geq 0.989$). The comparability in the tests with DEHS decreased when the spherical particle sizes exceeded 400 nm, which has been reported to be the upper limit for accurate measurement with this type of instruments. Levin *et al.* (2015) compared the particle sizing and counting of the FMPS, Electrical Low Pressure Impactor (ELPI, Dekati, Finland) and a Scanning Mobility Particle Sizer (SMPS) for spherical particles in the size range of 50–900 nm. While ELPI and SMPS data agreed well within the tested size-range, the FMPS was unable to size particle larger than 200 nm correctly. This led to it severely underestimating the particle size and overestimating the concentration.

Leavey *et al.* (2013) compared the Aerotrak with LDSA concentrations calculated from size distributions measured with a SMPS for a range of different particle types and morphologies with mean particle diameters ranging from 30 to 140 nm. They found a strong correlation (R^2 0.78–0.99) between the two methods but a moderate dependency on particle type. In most cases, the SMPS data overestimated the LDSA as compared to the Aerotrak. Leskinen *et al.* (2012) compared LDSA concentrations measured with NSAM and SMPS and found that for TiO_2 agglomerates and dust agglomerates and found that values from NSAM were higher than those of the SMPS.

Todea *et al.* (2015) compared the measured LDSA from Aerotrak and NSAM for monodisperse spheres and agglomerates with the calculated value based on number concentration from a Condensational Particle Counter (CPC) and knowledge of particle size. They found that for spherical particles the NSAM and Aerotrak data both generally agreed within ± 30% with the calculated value from the CPC in the size range of 20 to 346 nm. For spheres larger than 400 nm, LDSA concentration was underestimated by both instruments. For agglomerated particles, the instruments based on unipolar diffusion charging generally overestimated the LDSA concentration compared to the CPC value, but mostly still within ± 30%.

These previous results indicate that both method- and size-specific differences exist in the results given by different measurement devices used for sub-µm sized particles. Additional differences may arise when such devices are used to measure agglomerates with even wider size-distributions and different highly complex agglomerate structures, which may be found in dust generated from nanopowders. Since most applicable instrument(s), and potentially also the reliability of measurement results, will depend on the characteristics of the airborne particles and their size-distribution and all aerosol instruments in principle are calibrated and report their data assuming spherical equivalent diameters, it is difficult to measure and report true particle exposure values. This is because the assumptions required for generating the correct values are usually not known or are very complex in true exposure situations, and it is still poorly understood how instrument responses vary with the many different material characteristics and properties.

The aim of this study was to investigate the comparability of the results in a performance test of four commonly used

real-time monitoring particle measuring instruments when challenged to pigment and nanomaterial powder dusts which resemble dust from occupational powder handling. For comparison with a morphologically simple aerosol, we also demonstrate the performance of the measurement devices challenged to a spray product forming nm-size condensate particles (Norgaard *et al.*, 2009). Because all currently commercially available surface area monitors report the biologically relevant alveolar lung deposited surface area, this work also involves an analysis of potential procedures of conversion between measured number size distribution data and LDSA and their comparability. Finally, the real-time measurement data are compared with interpretations from gravimetric measurements of collected respirable dust samples.

The test powder materials were specifically selected to challenge the monitoring instruments based on their variations in primary particle size and specific surface areas as determined by the BET technique. Dust aerosols released from such powders may pose some measurement problems due to their level of agglomeration, size-distribution and multimodality, which may not be revealed in tests using standard testing particles such as PSL, NaCl or DEHS. However, documentation of these problems and their levels is important to understand the ability to use such instruments for monitoring and regulatory exposure assessment.

MATERIALS AND METHODS

Instrumentation

Four different real-time monitoring instruments were used in this study as listed below. Two of them are particle sizing instruments while the other two are LDSA concentration monitors. All instruments were calibrated by the manufactures prior to the study.

- **Fast Mobility Particle Sizer (FMPS; TSI model 3091, TSI Inc., Shoreview, MN, USA).** In the FMPS, particles are charged through a dual unipolar diffusion charger prior to size classification according to particles electrical mobility based on their trajectory in an electrical field. The electrical charge carried by the size classified particles is measured with 22 electrometers which currents are corrected for multiple charges and image charges and further inverted to size distribution having 32 bins between 5.6 and 560 nm. The FMPS was used to measure particle number size distributions. The alveolar deposited surface area concentration and respirable surface area concentration were further calculated assuming spherical particles with unit density. Sampling for the FMPs is done using a PM_1-cyclone to remove micron-sized particles.
- **Electrical Low Pressure Impactor (ELPI, Dekati, Finland).** In the ELPI (Keskinen *et al.*, 1992; Marjamaki *et al.*, 2005), particles are charged using a unipolar diffusion charger after which the particles are collected in a low pressure cascade impactor which fractionates the particle sizes based on their aerodynamic properties into 12 channels spanning from 30 nm to 10 μm. The electrometer detected current in each stage is corrected for multiple charges, image charges and inverted to a size distribution. In this study the ELPI was used to measure particle number size distributions and further calculate alveolar deposited surface area concentration and respirable surface area concentration.
- **Nanoparticle Surface Area Monitor (NSAM; TSI model 3550, TSI Inc., Shoreview, MN, USA).** The NSAM uses unipolar diffusion charging and a Faraday cup electrometer to measure a current which was found to be proportional to the lung deposited surface area concentration. By changing the voltage of the instrument ion trap, different proportionalities can be applied to mimic that of alveolar or tracheobronchial deposition as described by ICRP (1994). The inlet of the NSAM is mounted with a PM_1-cyclone. In this study, only the alveolar deposited surface area measured by the NSAM was investigated.
- **Aerotrak (Aerotrak 9000, TSI Inc., Shoreview, MN, USA).** The Aerotrak is a field-portable version of the NSAM. In all other functions it is identical to the NSAM. The inlet of the Aerotrak is mounted with a PM_1-cyclone. The Aerotrak has previously been compared with the NSAM and good agreement has been confirmed (Bau *et al.*, 2012).

Case of Spherical Particles Challenging the Instruments

The first experiment was carried out in a 20 m^3 stainless steel chamber which was ventilated using a HEPA-filtered outdoor air which was well mixed within the chamber using two fans. A well-studied surface cleaning and maintenance product Multicover (Nanocover, Denmark) was applied for 10 seconds from a distance of 20 cm onto a metal sheet (Norgaard *et al.*, 2009; Norgaard *et al.*, 2010). Approximately 5 minutes after spraying a nucleation event took place, which formed nm-size droplet particles anticipated to be due to nucleation through limonene oxidation that slowly grew in size through condensation.

Airborne particles were sampled from the room at the same point using separate conductive tubes for each instrument. The tube lengths were adjusted so that residence times were equal for each instrument to avoid differences in particle losses. As spray condensation particles are considered to be highly spherical, this experiment on one hand served as a calibration check of the instruments as well as a challenge to a simple aerosol within the optimum application ranges of all instruments.

Case of Dust Particles Challenging the Instruments

Seven different powders (Table 1) were selected so that primary particle sizes varied from 16 nm to over 100 nm, specific surface areas from 0.03 to 113 $m^2\ g^{-1}$, (Volume-Specific Surface Area (VSSA) from 0.3 to 437 $m^2\ cm^{-3}$ calculated using the nominal material densities from 2.7 to 10.4 g cm^{-3}). The variation in specific surface areas was used to indicate the potential level of aggregation in the powder particles. The extraordinary low specific surface area was observed for the PVP-stabilized AgNP powder, which appears as large aggregates with a water-soluble PVP matrix. The highest specific surface area material was UF TiO_2, which also had the smallest primary particle size (16 nm).

Table 1. Physico-chemical properties of powders.

Powder name	Producer	Reference Code (Producers names)	XRD-Structure	XRD size [nm]	Nominal Density [g cm^{-3}]	SSA [m^2 g^{-1}][a]	VSSA[b] [m^2 cm^{-3}]	Mass-loss[d] [wt%]	Organic coating
$CaCO_3$ #1	SkySpring Nanomaterials Inc, Houston, TX, USA	NRCWE-012 ($CaCO_3$ for water-based latex paint)	Calcite	73 ± 3	2.7	31.9	86	4	Fatty acid methyl ester
$CaCO_3$ #2	SkySpring Nanomaterials Inc, Houston, TX, USA	NRCWE-011 ($CaCO_3$)	Calcite	> 100	2.7	11.6	31	-	N/D
UF TiO_2	Kemira Oyj, Helsinki, Finland	UF TiO_2[e] (UV Titan M111)	Anatase	16 ± 1	3.9	112	437	4.5	N/D
TiO_2 AFDC	Kemira Oyj, Helsinki, Finland	TiO_2 AFDC[e] (TiO_2 AFDC)	Rutile	> 100	4.3	6.0	26	-	N/D
TiO_2 Pigment	NaBond Technologies Co., Ltd, Shenzhen, China	NRCWE-004 (Titanium oxide Nano-powder; Rutile-TiO_2)	Rutile	94 ± 4	4.3	9.7	42	-	N/D
ZnO	Umicore N.V. Brussels, Belgium	UMICORE ZANO[e] (ZANO)	Zincite	40 ± 1	5.6	22	123	-	N/D
AgNP	Nanogap sub-nm-powder, S.A., A Coruña, Spain	NRCWE-009 (NGAP NP)	Metallic	41 ± 2[c]	10.4[c]	0.03[c]	0.3[c]	15[c]	PVP[c]

[a] As measured with Krypton-BET on bulk material. [b] Estimated VSSA using nominal densities and neglecting the potential presence of organic-chemical surface modifications and coatings. [c]Data from Nymark *et al.* (2013). [d] Thermogravimetric analysis, 10 °C min^{-1} up to 1000°C. [e] Original sample name at the Finnish Institute of Occupational Health.

The powders were aerosolized using the miniaturized EN15051 dustiness drum (Schneider and Jensen 2008). The system has been made to correspond to the EN15051 standard drum so relative dimensions have been maintained and the 33 drops per minute is ensured by three lifter vanes in the drum and an 11 rpm rotation. The inlet air to the drum was controlled at 50% RH and HEPA-filtered to ensure a particle-free background. The measurements were split into two separate sampling trains in order to maintain 11 L min^{-1} flow through the drum (Fig. 1). Before starting the test, 2 g of powder was loaded into the drum, which was then rotated for 60 seconds to ensure that all surfaces were saturated with particles. After the drum had been emptied, 6 g of test material were loaded into it and 60 seconds of background measurements were done without the drum rotating to ensure a particle free test atmosphere. The experiment was then initiated by rotating the drum for 60 seconds during which particles were emitted and led through the airflow to the sampling train. After the drum was stopped, measurement of remaining airborne particles was conducted for another 120 seconds. This completed the rotational test. The measurement was then repeated an additional two times and the results here are presented as averages over the three experiments.

In the first experimental set-up (Fig. 1(a)), respirable dust (as defined by EN 481 (1993), D_{50} = 4 μm) was collected with a GK2.69 cyclone at 4.2 L min^{-1} (BGI Inc., Waltham, MA, USA), and particle concentrations were measured with the FMPS, NSAM and Aerotrak. In addition, an Electrostatic Precipitator (ESP, Asbach, 2015) was used to deposit particles onto 25 mm silica wafers. These were then used in an un-coated state for analysis by Scanning Electron Microscopy (SEM) using a FEI ESEM Quanta 200 FEG (FEI, Eindhoven, the Netherlands) and Energy-Dispersive X-ray Spectroscopy (EDX) to ensure that the particles of interest were studied. The respirable dust mass was determined using a Sartorius microbalance (Type R162 P; Sartorius GmbH, Göttingen, Germany), after conditioning the filters and control filters in a weighing room (22°C; 50%RH) before and after sampling. The measured mass was used to calculate the gravimetrical powder dustiness index and categorize the powder dustiness level according to EN15051.

In the second experimental set-up (Fig. 1(b)), particle size distributions were measured by using the ELPI and FMPS. The FMPS was used to validate that the measurements were comparable with the measurements performed in the first experimental set-up.

Particle Concentrations Analysis

1) Comparison of LDSA Concentrations

For both FMPS and ELPI, alveolar particle number concentration fractions were calculated by multiplying measured particle number size distributions with the alveolar deposition fraction, DF_{alv} (ICRP, 1994). The alveolar deposition fraction is based on aerodynamic diameter; therefore we assumed spherical particle shape and unit density while calculating the FMPS alveolar particle number concentrations. Particle number size distributions measured

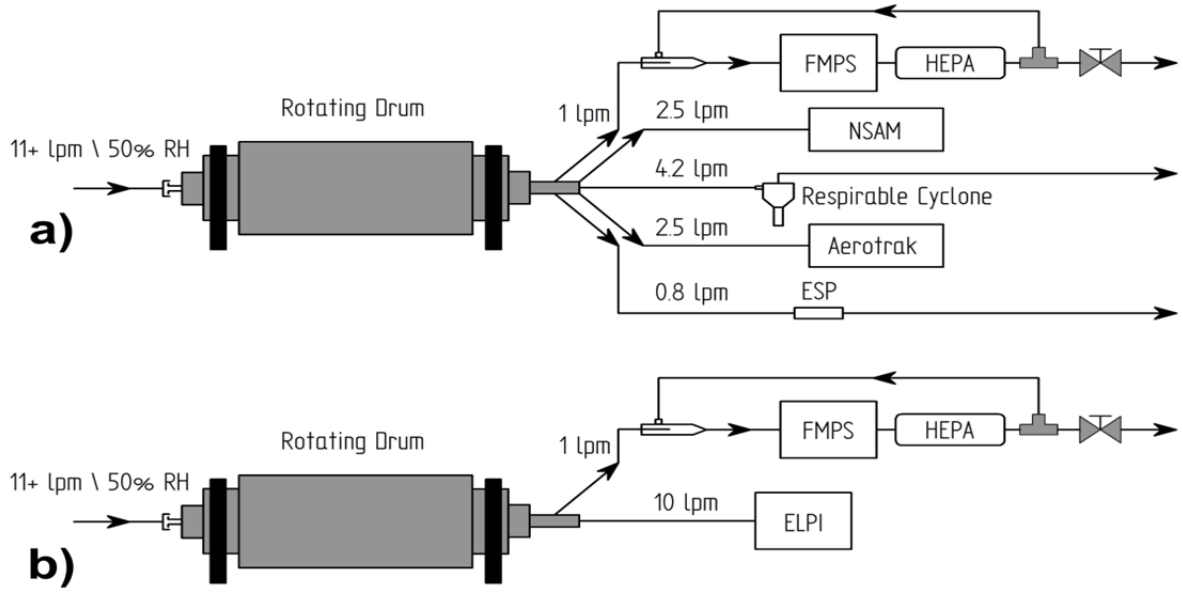

Fig. 1. Schematic overview of measurement setups connected to dustiness drum.

by the ELPI were also multiplied with the NSAM PM_1-cyclone penetration efficiency (Table S1) to simulate the cyclone placed upstream of the NSAM, Aerotrak and FMPS. For direct comparison of the measured LDSA concentrations between the 4 instruments, time series data were converted into running 5 second averages. Due to NSAM and Aerotrak measuring alveolar deposited surface area, $LDSA_{alv}$, the ELPI and FMPS (without PM_1 fractions) had to be recalculated according to:

$$LDSA_{alv} = \pi \sum D_p n(D_p) \cdot D_p^2 \cdot DF_{alv}(D_p) \cdot PM_1(D_p) \ [m^2] \quad (1)$$

with $n(D_p)$ being the number of particles with diameter D_p, DF_{alv} and PM_1 being the alveolar deposition fraction and cyclone penetration fraction for the specific particle size, respectively.

2) Comparison of Respirable Surface Area Concentrations

A second analysis was completed to investigate the comparability between the theoretical geometric surface area of the respirable dust collected on the filter for dustiness categorization and the theoretical accumulated respirable surface area concentrations of the airborne dusts measured with the FMPS and ELPI.

On the one hand, respirable LDSA values were compared with the respirable particle surface area calculated from the respirable gravimetric measurements [g] multiplied by their respective specific surface areas [$m^2\ g^{-1}$] (Table 1).

On the other hand, FMPS and ELPI particle number size distributions were converted to geometric surface area size distributions, assuming spherical particles (SA_{sph}). The latter is then integrated during the sampling period (180 s), and, transformed to the corresponding respirable fractions, *RF*. It should be noted that the FMPS was included in comparison, despite not covering the entire range of the respirable fraction. It is therefore expected that the FMPS data will underestimate the surface area in cases where a considerable number of particles are larger than 560 nm.

$$SA_{sph} = \pi \cdot \frac{Q_{drum}^2}{Q_{instr}} \cdot \int_0^{\tau} \sum_{D_p} \left[n\left(D_p, t\right) \cdot D_p^2 \cdot RF\left(D_p\right) \right] dt \quad (2)$$

where $n(D_p, t)$ is the number size distribution (FMPS, ELPI) at time t, Q_{drum} the total air flowrate of the drum, Q_{instr} the instrument flow and τ the sampling time.

Another approach is based on particle volume size distribution, combined with the respirable fraction, material density, ρ, and specific surface area, *SSA*:

$$SA_{ssa} = \frac{\pi}{6} \cdot \rho \cdot SSA \cdot \frac{Q_{drum}^2}{Q_{instr}} \cdot \int_0^{\tau} \sum_{D_p} \left[n\left(D_p, t\right) \cdot D_p^3 \cdot RF\left(D_p\right) \right] dt \quad (3)$$

Unlike the first approach this uses the assumption of spherical shape to calculate a total volume which then is recalculated into a surface area using known properties of the material.

RESULTS AND DISCUSSION

Dustiness

Fig. 2 shows an overview of the measured gravimetrical respirable dustiness indices for the 7 materials used in the study along with the regions of classification of powder dustiness according to EN15051. The materials covers a wide range of dustiness from *Very Low* (TiO_2 Pigment, TiO_2 AFDC, $CaCO_3$ #2) to *Low* (AgNP) and *High* (ZnO, $CaCO_3$ #1, UF TiO_2).

Real-Time Measurements

Particle size distribution measurements by the FMPS and ELPI showed a good agreement on the droplets formed

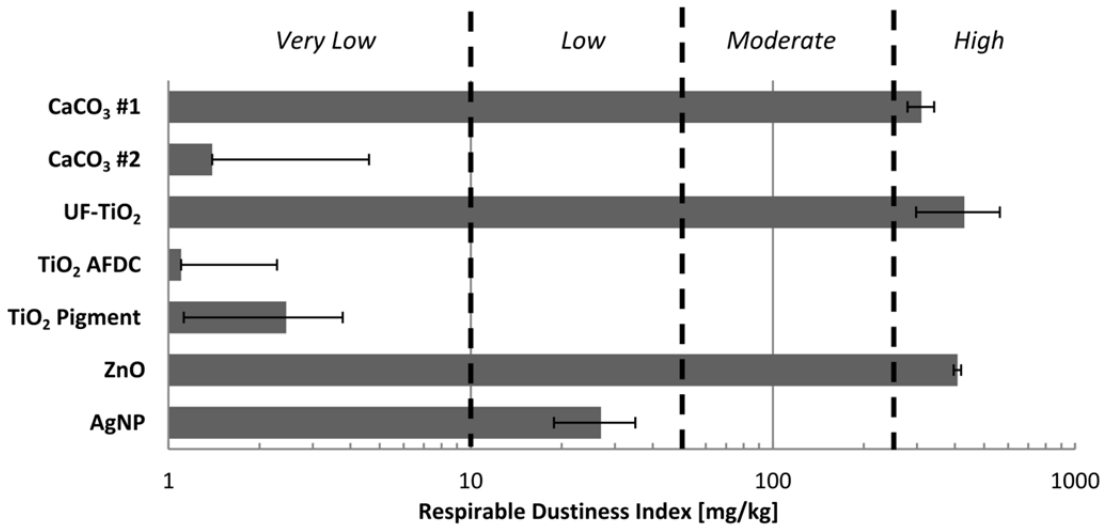

Fig. 2. Measured dustiness indices and classification regions according to EN15051. Whiskers denote one standard deviation.

in the chamber measurements (Fig. 3(a)). The small rotating drum shows in general good repeatability even though differences may occur in the modal diameter as well as the shape of the (number size) distribution. However, large discrepancies/deviations between FMPS and ELPI number size distributions were observed for all non-spherical powder particles generated using the small rotating drum (Figs. 3(b)–3(h)). More precisely, the FMPS shows consistently higher particle number concentrations within its measurement size range (< 560 nm) as compared to the ELPI. In the FMPS, particle concentrations often abruptly decreased in particle sizes below 100 nm (Figs. 3(a), 3(b), 3(d), 3(g), and 3(h)) while particles concentrations were specifically predominant in the size region of 150–200 nm. On contrary, the ELPI did not show any increased particle concentrations in this size range (Figs. 3(b)–3(h)). For powders, the ELPI peak particle number concentrations were generally located in the size range of 0.5 to 2 µm. It should be remembered that the FMPS classifies particles according to their *electrical mobility equivalent* diameter while the ELPI measures *aerodynamic equivalent diameter*, which are equal if particles are spherical and have unit density (1 g cm^{-3}). In the chamber experiment, particles are presumably spherical with a density close to 1 g cm^{-3}. Thus, the FMPS and ELPI particle number size distributions were found to be similar (Fig. 3(a)). However, in the rotating drum experiments, airborne particles are highly agglomerated, with particle effective densities that are likely to be significantly different from unity. For powder particles, an order of magnitude difference in measured modal diameter was observed. This difference cannot be explained alone by particles shape and density; it would require two orders of magnitude difference in effective density as estimated by using the relation between the mobility diameter and aerodynamic diameter as described by Kelly and McMurray (1992). The deviating FMPS measurement is explained by Levin *et al.* (2015) where it is shown that FMPS is unable to measure distributions of spherical particles with a Geometric Mean Diameter (GMD) higher than 200 nm. This is partly because the electrical mobility size dependency flattens out within the FMPS size range and particles become harder to size-separate based on this technique. Furthermore, secondary effects in the FMPS current inversion seem to affect the final size distribution. For distributions having a GMD above 200 nm, it still shows them as having a GMD of 200–300 nm, and overestimates the number concentration. Furthermore, Shin *et al.* (2010) showed that agglomerated particles have higher unipolar charging efficiency than spherical particles having the same mechanical mobility. Thus, after unipolar charging, the electrical mobility of an agglomerate is higher than the electrical mobility of a spherical particle having equivalent mechanical mobility as the agglomerate. Increased agglomeration level is seen in the FMPS measurements as a decrease in electrical mobility size and an increase in concentration. It also moves the minima in electrical mobility into the FMPS size range, making size-classification based on this ambiguous (Levin *et al.*, 2015). In the ELPI measurements, agglomeration increases the measured concentration due to increased charging capabilities.

Electron Microscopy

Typical dust particles from each material used in the dustiness drum and collected using the ESP is shown in Fig. 4. The AgNP appears in irregular aggregates with no clear primary particles visible by SEM (Fig. 4(g)) while other powder particles appear as aggregates of fused primary particles. The special appearance of the AgNP is explained by the abundant matrix encapsulating the AgNP (see Nymark *et al.* (2013) for TEM images of the primary AgNP particles). It was impossible to generate statistical data on particle size-distributions and morphologies due to insufficient number of particle counts on the images obtained. However, qualitatively, the fractal dimensions of the particles studied are all rather close to 3, which correspond to compact particles (Virtanen *et al.*, 2004). This would mean that the unipolar charging done in the instruments should not be affected too much by the particle morphology.

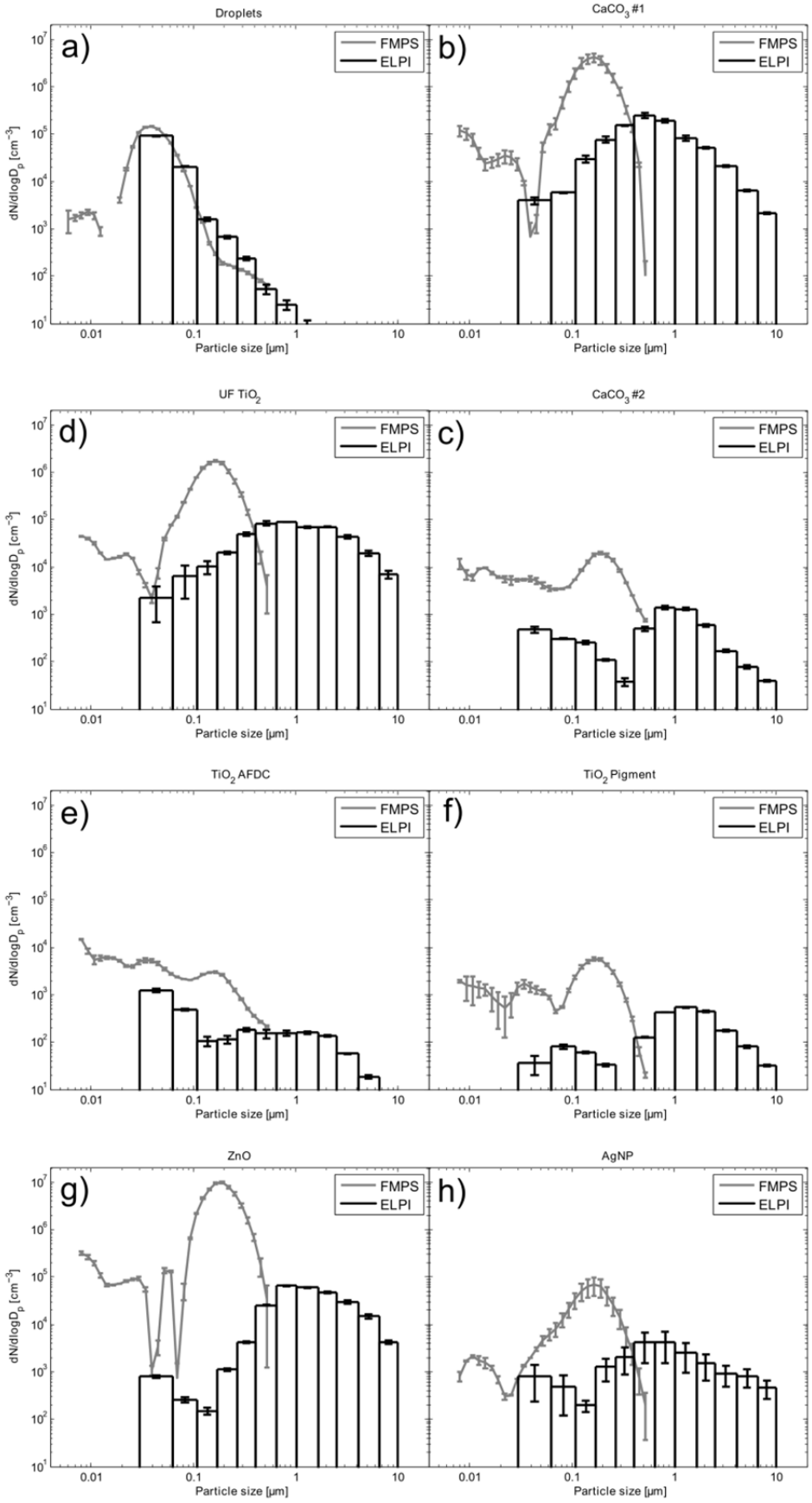

Fig. 3. Size distributions of sprayed droplets (a) and seven materials form the dustiness drum (b)–(h) as measured by FMPS and ELPI.

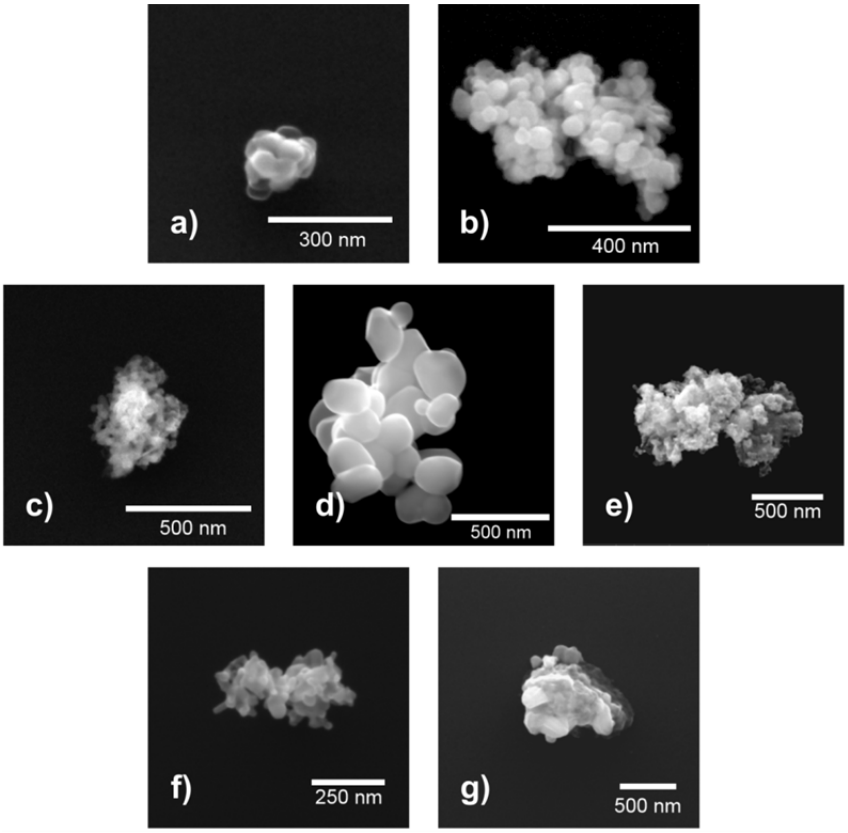

Fig. 4. SEM images of a) $CaCO_3$ #1 b) $CaCO_3$ #2 c) UF TiO_2 d) TiO_2 AFDC e) TiO_2 Pigment f) ZnO g) AgNP.

Surface Area Comparison

The first step in the comparison was a benchmark comparison between the NSAM and Aerotrak, which are specifically designed for LDSA concentration measurements. Since both instruments are based on the same design, they were expected to give very similar results. Fig. 5(a) shows the LDSA concentration measured by the NSAM plotted against that of Aerotrak for all test particles. The LDSA concentration measured from spherical test particles was well within the manufacturer's given accuracy (both instruments are specified to have a ± 20% measurement accuracy in the region of 20 to 200 nm) and had an average ratio of 1.06 (Table 2). In general the surface area monitors showed good comparability with a few exceptions. For low surface area materials, $CaCO_3$ #2 and TiO_2 Pigment, the Aerotrak gave notably higher concentrations of surface area and the correlation between the instruments was poor. TiO_2 AFDC, while having a poor correlation, gave values within ± 20% of the NSAM. For the powders with higher specific surface area, the Aerotrak appears to give slightly higher values than NSAM, but with better correlation factors. This shows that, even though the instruments are based on the same principle, the response to various particle shapes may differ. This may be due to differences in charger ion concentration and following calibration factors.

The calculated LDSA concentration measured using FMPS data are shown in Fig. 5(b), with correlation factors and ratios in Table 2. It shows that the LDSA concentration measured using the FMPS appears to correlate well with that of the NSAM for certain powder materials such as $CaCO_3$ #1, ZnO, AgNP and UF-TiO_2 throughout their whole spectra of LDSA concentration levels. For most powders the FMPS appears to consequently give higher values than the NSAM, with the exceptions of UF-TiO_2 where the ratio is 0.77. The disagreement between the methods increases slightly at lower surface areas, i.e., for TiO_2 Pigment. No powder material has an average ratio within the ± 20% boundaries. The underestimation of the NSAM as compared to the FMPS could be explained by the fact that NSAM underestimates LDSA concentrations for particles larger than 400 nm (Asbach *et al.*, 2009). The assumption of spherical particle shape and unit density could also affect the results.

The LDSA concentration of particles below the 1 μm cut-off measured with the ELPI is shown in Fig. 5(c). The correlation of LDSA concentrations between the ELPI calculated values and the NSAM was fair (R^2 0.87–0.93) for the high surface area powders but poorer (R^2 0.5–0.72) for the low surface area ones (Table 2). The ELPI calculated LDSA concentrations were underestimated as compared to the ones measured by the NSAM. Only UF-TiO_2 has an average ratio within the ± 20% boundary. It should be noted that the ELPI was not measuring on the same aerosol as the surface area monitors but on separate repetitions of the same experiment, due to limitations in the total available volume-flow through the drum. However, measurements done with FMPS during both setups showed a good comparability between the two setups ($R^2 > 0.95$).

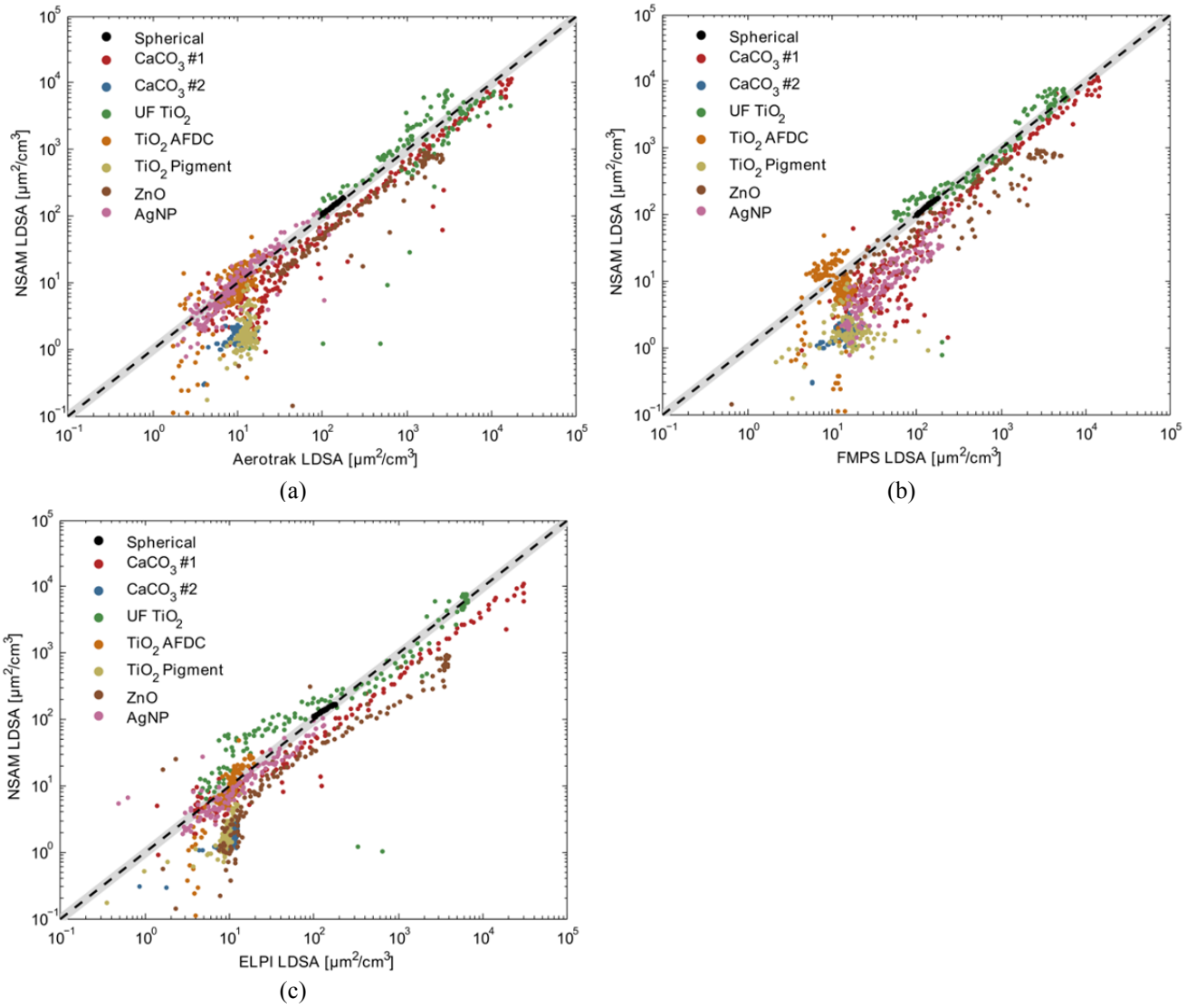

Fig. 5. Comparison alveolar deposited surface area measured by NSAM and (a) Aerotrak, (b) FMPS, and (c) ELPI. Grey area denotes ± 20% uncertainty.

Table 2. Correlation coefficients and ratios between LDSA determined by Aerotrak, FMPS and ELPI against NSAM.

Instrument	Aerotrak		FMPS		ELPI	
Material	R^2	Ratio	R^2	Ratio	R^2	Ratio
Droplets	0.99	1.06 ± 0.01	0.99	1.01 ± 0.01	0.98	1.03 ± 0.04
$CaCO_3$ #1	0.96	1.68 ± 0.2	0.97	1.51 ± 0.27	0.93	2.14 ± 0.11
$CaCO_3$ #2	0.34	6.97 ± 0.03	0.26	10.05 ± 0.01	0.53	6.17 ± 0.03
UF TiO_2	0.73	2.81 ± 0.7	0.89	0.77 ± 0.08	0.92	1.12 ± 0.48
TiO_2 AFDC	0.45	1.18 ± 0.4	0.37	1.77 ± 1.08	0.72	2.84 ± 2.46
TiO_2 Pigment	0.05	7.12 ± 1.2	0.01	11.23 ± 0.76	0.50	4.43 ± 0.63
ZnO	0.94	2.40 ± 0.4	0.93	3.29 ± 1.71	0.93	5.19 ± 0.44
AgNP	0.74	1.04 ± 0.04	0.96	4.38 ± 1.88	0.87	1.35 ± 0.294

Fig. 6 shows that the accumulated respirable dust surface area calculated from gravimetric samples and calculated using Eqs. (2) and (3) from the ELPI and FMPS measurements were only similar for a few powders. With the exception of AgNP, the respirable dust surface areas calculated directly by assumption of spherical particles (Eq. (2)) is greatly underestimated as compared to the respirable dust surface area assigned from gravimetric measurements. This exception is likely due to its very low SSA as a bulk material. When the specific density and SSA is considered (Eq. (3)) the values for airborne dust as measured by the ELPI generally correlates well with the values for filter-based calculations

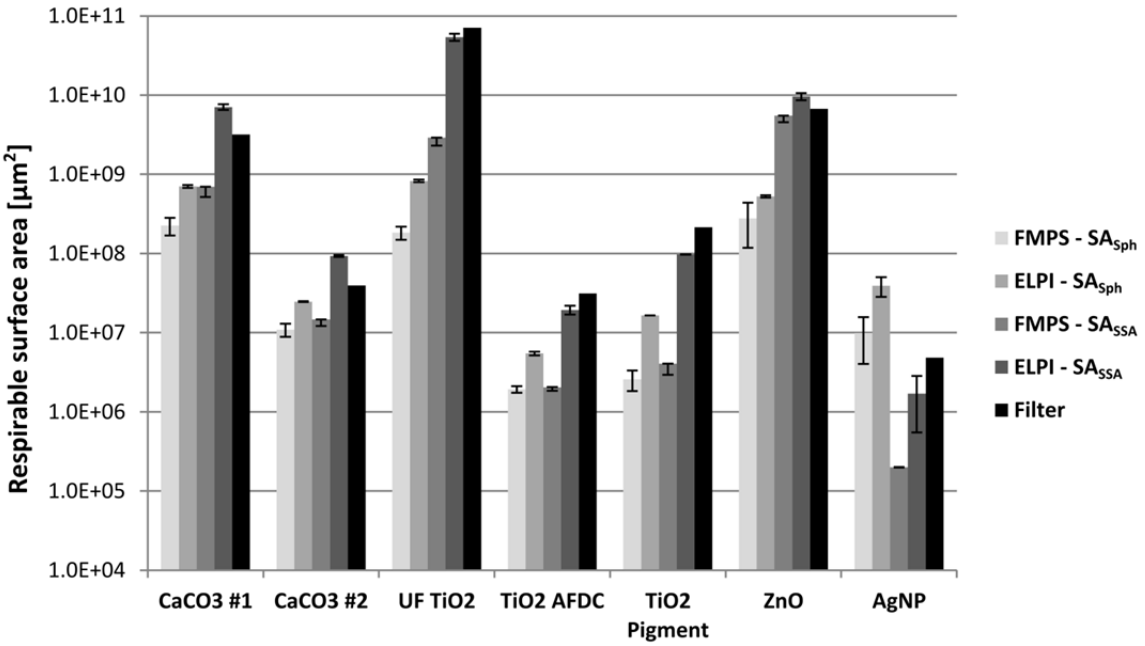

Fig. 6. Calculated respirable fraction surface area from FMPS, ELPI as described in Eqs. (2) and (3), and calculated value from filter sampling.

(R^2 0.98, Ratio 1.17). The corresponding values for the FMPS do not have a general trend towards approaching the gravimetrical value (Ratio 0.23). From this it is evident that using the relative density in the assessment of airborne dust surface area measured with the ELPI improves the comparability with the surface area derived from the respirable dust mass. However, large differences between the two estimates of released dust surface area may still arise for certain materials.

CONCLUSIONS

This study analyzes the comparability of lung deposited surface area (LDSA) concentrations as measured by or derived from four commonly used devices and approaches (FMPS, ELPI, NSAM, and Aerotrak) for both spherical particles and seven different powders aerosolized using the small rotary drum to simulate realistic workplace-like nanostructured dust particles. Test aerosol LDSA concentrations ranged from 0.1 to 10^4 µm^2 cm^{-3} as measured by NSAM, where spherical particles were mainly below 100 nm, while powder-borne particles covered the range from 0.1 to 10 µm, based on ELPI measurements. Powders dustiness indices varied from *Very Low* up to *High* according to the EN:15051 classification.

Test of spherical droplets after application of a surface coating product showed a good correlation (R^2 > 0.97, Ratio between 1.0 and 1.04) between NSAM, FMPS and Aerotrak for alveolar LDSA.

Dustiness testing of the seven highly different powders showed only fairly reliable correlation (R^2 between 0.73 and 0.93) and concentration ratio (1.04–2.8) between the two surface area monitors tested for the high surface area range of materials. However, the comparison was inconsistent for the lower surface area concentrations and varied considerably. Similar levels of correlation were observed comparing the data from the NSAM and the FMPS for high surface area materials, but with the FMPS overestimating the concentration. Finally, the re-calculated ELPI LDSA concentrations showed good correlation at high concentrations (R^2 between 0.87 and 0.93), with somewhat lower correlation at the lower end (R^2 between 0.50 and 0.72). The LDSA concentration ratios were between 1.12 to 5.19 and 1.35 to 4.43, respectively.

Using a different approach, we evaluated the comparability between accumulated surface areas derived from on-line particle size-distribution measurements using FMPS and ELPI and a theoretical respirable dust surface area calculated based on the mass of respirable dust collected on filters. The results show that dust surface area converted from ELPI data may generally correlate well (R^2 > 0.98, Ratio 1.17) with the theoretical mass-based surface area of the generated dust particles. However, some large deviations were observed for the same calculations using FMPS data which may be due to particle morphology (agglomeration/aggregates), effective densities, and other previously mentioned issues regarding online measurement of particle size-distributions and surface areas. Further studies are required to validate the results using this approach for assessment of airborne dust particle LDSA with ELPI as it shows promise.

As an over-arching conclusion, the measured LDSA concentrations variation between the instruments exceeded any accepted limit for comparability between the instruments and was strongly material dependent. The observed lack of data agreement between the different state-of-the-art measurement equipment is important and the apparent discrepancies encourage the need for further metrological research. If LDSA is to become a metric of choice in

toxicology and occupational exposure assessments as well as regulatory enforcement, then a method of choice has to be decided or developed as current techniques give material dependent results and do not have the appropriate comparability. Results from different techniques can therefore not be trusted to represent comparable levels of LDSA concentrations. The results should have implications for development of new measurement devices developed.

ACKNOWLEDGEMENTS

This work was conducted as part of the Strategic Research effort at the National Research Centre for the Working Environment and the 'Danish Centre for Nanosafety' (20110092173/3) from the Danish Working Environment Research Foundation, and the EU Framework 7 Programme NANODEVICE (NMP4-LA-2009-211464). We thank Signe H. Nielsen for technical assistance during dustiness testing and being responsible for gravimetric measurements of filters from dustiness testing and FIOH for donation of the samples in connection with the NANODEVICE project.

SUPPLEMENTARY MATERIALS

Supplementary data associated with this article can be found in the online version at http://www.aaqr.org.

REFERENCES

Aitken, R.A., Bassanm A., Friedrichsm S., Hankin, S.M., Hansen, S.F., Holmqvist, J., Peters, S.A.K., Poland, C.A. and Tran, C.L. (2011). Specific Advice on Exposure Assessment and Hazard/Risk Characterisation for Nanomaterials under REACH (RIP-oN 3).

Asbach, C., Fissan, H., Stahlmecke, B., Kuhlbusch, T.A.J. and Pui, D.Y.H. (2009). Conceptual limitations and extensions of lung-deposited Nanoparticle Surface Area Monitor (NSAM). *J. Nanopart. Res.* 11:101–109.

Asbach, C., Kaminski, H., von Barany, D., Kuhlbusch, T.A., Monz, C., Dziurowitz, N., Pelzer, J., Vossen, K., Berlin, K., Dietrich, S., Gotz, U., Kiesling, H.J., Schierl, R. and Dahmann, D. (2012). Comparability of portable nanoparticle exposure monitors. *Ann. Occup. Hyg.* 56: 606–621, doi: 10.1093/annhyg/mes033

Asbach, C. (2015). Exposure Measurement at Workplaces, In *NanoEngineering – Global Approaches to Health and Safety Issues*, by Dolez, P. (Ed.), Elsevier Publishing, pp. 523–555.

Bau, S., Witschger, O., Gensdarmes, F., Rastoix, O. and Thomas, D. (2010). A TEM-based method as an alternative to the BET method for measuring off-line the specific surface area of nanoaerosols. *Powder Technol.* 200: 190–201, doi: 10.1016/j.powtec.2010.02.023.

Bau, S., Witschger, O., Gensdarmes, F. and Thomas, D. (2012). Evaluating three direct-reading instruments based on diffusion charging to measure surface area concentrations in polydisperse nanoaerosols in molecular and transition regimes. *J. Nanopart. Res.* 14: 1217, doi: 10.1007/s11051-012-1217-6.

BS EN:481 (1993). Workplace Atmospheres. Size Fraction Definitions for Measurement of Airborne Particles.

BS EN:15051 (2006). EN15051 Workplace Atmospheres: Measurement of the Dustiness of Bulk Materials - Requirements and Reference Test Methods.

Donaldson, K., Schinwald, A., Murphy, F., Cho, W.S., Duffin, R., Tran, L. and Poland, C. (2013). The biologically effective dose in inhalation nanotoxicology. *Acc. Chem. Res.* 46: 723–732, doi: 10.1021/ar300092y.

Duffin, R., Tran, L., Brown, D., Stone, V. and Donaldson, K. (2007). Proinflammogenic effects of low-toxicity and metal nanoparticles in vivo and in vitro: Highlighting the role of particle surface area and surface reactivity. *Inhalation Toxicol.* 19: 849–856, doi: 10.1080/08958370701479323.

Fissan, H., Neumann, S., Trampe, A., Pui, D.Y.H. and Shin, W.G. (2006). Rationale and principle of an instrument measuring lung deposited nanoparticle surface area. *J. Nanopart. Res.* 9: 53–59, doi: 10.1007/s11051-006-9156-8.

Fissan, H., Kaminski, H., Asbach, C., Pui, D. and Wang, J. (2013). Rationale for data evaluation of the size distribution measurements of agglomerates and aggregates in gases with extended SMPS-technology. *Aerosol Air Qual. Res.* 13: 1393–1403, doi: 10.4209/aaqr.2013.02.0050.

Giechaskiel, B., Alfoeldy, B. and Drossinos, Y. (2009). A metric for health effects studies of diesel exhaust particles. *J. Aerosol Sci.* 40: 639–651, doi: 10.1016/j.jaerosci.2009.04.008.

Hämeri, K., Lähde, T., Hussein, T., Koivisto, J. and Savolainen, K. (2009). Facing the key workplace challenge: Assessing and preventing exposure to nanoparticles at source. *Inhalation Toxicol.* 21: 17–24, doi: 10.1080/08958370902942525.

Ibaseta, N. and Biscans, B. (2007). Ultrafine aerosol emission from the free fall of TiO_2 and SiO_2 nanopowders. *Kona Powder Part. J.* 25: 190–204.

ICRP (1994). Human Respiratory Tract Model for Radiological Protection.

Jacobsen, N.R., Moller, P., Jensen, K.A., Vogel, U., Ladefoged, O., Loft, S. and Wallin, H. (2009). Lung inflammation and genotoxicity following pulmonary exposure to nanoparticles in $ApoE^{-/-}$ mice. *Part. Fibre Toxicol.* 6: 2, doi: 10.1186/1743-8977-6-2.

Jensen, K.A., Koponen, I.K., Clausen, P.A. and Schneider, T. (2009). Dustiness behaviour of loose and compacted bentonite and organoclay powders: What is the difference in exposure risk? *J. Nanopart. Res.* 11: 133–146.

Jensen, K.A., Levin, M. and Witschger, O. (2015). Methods for Testing Dustiness, In *Nanomaterial Characterization: An introduction*m Tantra, R. (Ed.) John Wiley & Sons Inc.

Kelly, W. and Mcmurry, P. (1992). Measurement of particle density by inertial classification of differential mobility analyzer generated monodisperse aerosols. *Aerosol Sci. Technol.* 17: 199–212, doi: 10.1080/02786829208959571.

Keskinen, J., Pietarinen, K. and Lehtimaki, M. (1992). Electrical low-pressure impactor. *J. Aerosol Sci.* 23: 353–360, doi: 10.1016/0021-8502(92)90004-F.

Koivisto, A.J., Lyyranen, J., Auvinen, A., Vanhala, E., Hameri, K., Tuomi, T. and Jokiniemi, J. (2012). Industrial

worker exposure to airborne particles during the packing of pigment and nanoscale titanium dioxide. *Inhalation Toxicol.* 24: 839–849, doi: 10.3109/08958378.2012.724474.

Koivisto, A.J., Jensen, A.C., Levin, M., Kling, K.I., Maso, M.D., Nielsen, S.H., Jensen, K.A. and Koponen, I.K. (2015). Testing the near field/far field model performance for prediction of particulate matter emissions in a paint factory. *Environ. Sci. Processes Impacts* 17: 62–73, doi: 10.1039/c4em00532e.

Koponen, I.K., Koivisto, A.J. and Jensen, K.A. (2015). Worker exposure and high time-resolution analyses of process-related submicrometre particle concentrations at mixing stations in two paint factories. *Ann. Occup. Hyg.* 59: 749–763, doi: 10.1093/annhyg/mev014.

Leavey, A., Fang, J., Sahu, M. and Biswas, P. (2013). Comparison of measured particle lung-deposited surface area concentrations by an Aerotrak 9000 using size distribution measurements for a range of combustion aerosols. *Aerosol Sci. Technol.* 47: 966–978, doi: 10.1080/02786826.2013.803018.

LeBouf, R.F., Ku, B.K., Chen, B.T., Frazer, D.G., Cumpston, J.L. and Stefaniak, A.B. (2011a). Measuring surface area of airborne titanium dioxide powder agglomerates: Relationships between gas adsorption, diffusion and mobility-based methods. *J. Nanopart. Res.* 13: 7029–7039, doi: 10.1007/s11051-011-0616-4.

Lebuf, R.F., Stefaniak, A.B., Chen, B.T., Frazer, D.G. and Virji, M.A. (2011b). Measurement of airborne nanoparticle surface area using a filter-based gas adsorption method for inhalation toxicology experiments. *Nanotoxicology* 5: 687–699, doi: 10.3109/17435390.2010.546951.

Leskinen, J., Joutsensaari, J., Lyyränen, J., Koivisto, J., Ruusunen, J., Järvelä, M., Tuomi, T., Hämeri, K., Auvinen, A. and Jokiniemi, J. (2012). Comparison of nanoparticle measurement instruments for occupational health applications. *J. Nanopart. Res.* 14: 718, doi: 10.1007/s11051-012-0718-7.

Levin, M., Koponen, I.K. and Jensen, K.A. (2014). Exposure assessment of four pharmaceutical powders based on dustiness and evaluation of damaged HEPA filters. *J. Occup. Environ. Hyg.* 11: 165–177, doi: 10.1080/15459624.2013.848038

Levin, M., Gudmundsson, A., Pagels, J.H., Fierz, M., Mølhave, K., Löndahl, J., Jensen, K.A. and Koponen, I.K. (2015). Limitations in the use of unipolar charging for electrical mobility sizing instruments: A study of the fast mobility particle sizer. *Aerosol Sci. Technol.* 49: 556–565, doi: 10.1080/02786826.2015.1052039.

Makela, J.M., Aromaa, M., Rostedt, A., Krinke, T.J., Janka, K., Marjamaki, M. and Keskinen, J. (2009). Liquid flame spray for generating metal and metal oxide nanoparticle test aerosol. *Hum. Exp. Toxicol.* 28: 421–431, doi: 10.1177/0960327109105154.

Marjamaki, M., Lemmetty, M. and Keskinen, J. (2005). ELPI response and data reduction - I: Response functions. *Aerosol Sci. Technol.* 39: 575–582, doi: 10.1080/027868291009189.

Maynard, A.D. and Kuempel, E.D. (2005). Airborne nanostructured particles and occupational health. *J. Nanopart. Res.* 7: 587–614.

Norgaard, A.W., Jensen, K.A., Janfelt, C., Lauritsen, F.R., Clausen, P.A. and Wolkoff, P. (2009). Release of VOCs and particles during use of nanofilm spray products. *Environ. Sci. Technol.* 43: 7824–7830, doi: 10.1021/es9010468

Norgaard, A.W., Larsen, S.T., Hammer, M., Poulsen, S.S., Jensen, K.A., Nielsen, G.D. and Wolkoff, P. (2010). Lung damage in mice after inhalation of nanofilm spray products: the role of perfluorination and free hydroxyl groups. *Toxicol. Sci.* 116: 216–224, doi: 10.1093/toxsci/kfq094.

Nymark, P., Catalan, J., Suhonen, S., Jarventaus, H., Birkedal, R., Clausen, P.A., Jensen, K.A., Vippola, M., Savolainen, K. and Norppa, H. (2013). Genotoxicity of polyvinylpyrrolidone-coated silver nanoparticles in BEAS. *Toxicology* 313: 38–48, doi: 10.1016/j.tox.2012.09.014.

Oberdorster, G. (2000) .Toxicology of Ultrafine Particles: in Vivo Studies. *Philos. Trans. R. Soc. London, Ser. A* 358: 2719–2739, doi: 10.1098/rsta.2000.0680.

Saber, A.T., Jacobsen, N.R., Jackson, P., Poulsen, S.S., Kyjovska, Z.O., Halappanavar, S., Yauk, C.L., Wallin, H. and Vogel, U. (2014). Particle-induced pulmonary acute phase response may be the causal link between particle inhalation and cardiovascular disease. *Wiley Interdiscip. Rev. Nanomed. Nanobiotechnol* 6: 517–531, doi: 10.1002/wnan.1279.

Schneider, T. and Jensen, K.A. (2008). Combined single-drop and rotating drum dustiness test of fine to nanosize powders using a small drum. *Ann. Occup. Hyg.* 52: 23–24.

Schneider, T., Brouwer, D.H., Koponen, I.K., Jensen, K.A., Fransman, W., Van Duuren-Stuurman, B., Van Tongeren, M. and Tielemans, E. (2011). Conceptual model for assessment of inhalation exposure to manufactured nanoparticles. *J. Exposure Sci. Environ. Epidemiol.* 21: 450–463.

Shin, W.G., Pui, D.Y.H., Fissan, H., Neumann, S. and Trampe, A. (2006). Calibration and numerical simulation of nanoparticle surface area monitor (TSI model 3550 NSAM). *J. Nanopart. Res.* 9: 61–69, doi: 10.1007/s11051-006-9153-y.

Shin, W.G., Wang, J., Mertler, M., Sachweh, B., Fissan, H. and Pui, D.Y.H. (2010). The effect of particle morphology on unipolar diffusion charging of nanoparticle agglomerates in the transition regime. *J. Aerosol Sci.* 41: 975–986, doi: 10.1016/j.jaerosci.2010.07.004.

Todea, A.M., Beckmann, S., Kaminski, H. and Asbach, C. (2015). Accuracy of electrical aerosol sensors measuring lung deposited surface area concentrations. *J. Aerosol Sci.* 89: 96–109.

Tsai, C.J., Wu, C.H., Leu, M.L., Chen, S.C., Huang, C.Y., Tsai, P.J. and Ko, F.H. (2009). Dustiness test of nanopowders using a standard rotating drum with a modified sampling train. *J. Nanopart. Res.* 11: 121–131.

Virtanen, A., Ristimaki, J. and Keskinen, J. (2004). Method for measuring effective density and fractal dimension of

aerosol agglomerates. *Aerosol Sci. Technol.* 38: 437–446, doi: 10.1080/02786820490445155.

Received for review, June 22, 2015
Revised, October 12, 2015
Accepted, October 12, 2015